Model for Colloidal Fouling of Membranes

P. Bacchin, P. Aimar, and V. Sanchez

Lab. de Génie Chimique et Electrochimie, 31062 Toulouse, Cedex, France

A proposed theoretical model describes colloids deposition on a membrane surface accounting for surface interactions. A mass-transfer equation links the deposition rate to hydrodynamic conditions (permeation and tangential flow through a boundary layer thickness, δ) and to physicochemical properties of the suspension (diffusion, D, and potential barrier between particles, V_B). This equation predicts the existence of a critical flux, J_{crit}, for ultrafiltration, reverse osmosis, or microfiltration of large-size colloids as:

$$J_{crit} = \frac{D}{\delta} \, ln\left(\frac{V_B}{\delta}\right)$$

Some of the trends observed when processing protein solutions are explained by this model. Previous experimental data for various colloids or our data with a clay suspension in the presence of electrolytes are also compared to predictions of our model. It explains the "flux anomaly" for particle sizes between 10 nm and 1 μm.

Introduction

Microfiltration (MF), ultrafiltration (UF), and reverse osmosis (RO) are pressure-driven membrane separation processes whose major limitation is fouling. Solutions treated by these systems are often composed largely of colloids. The term colloid covers various species with particles smaller than 5 μm, stable in suspension or charged macrosolutes such as proteins.

For a colloid, surface electrostatic interactions play an important role. With diffusion, these interactions control the rate of coagulation (Verwey and Overbeek, 1948) and the variation in diffusivity with concentration (Anderson et al., 1978). The physical adsorption of a solute on a surface is also the consequence of such interactions together with diffusion and hydrodynamics (Rajagopalan and Kim, 1981). (The concepts of deposition, adhesion, and adsorption are similar; the first term seems more appropriate for colloidal particles and the third one for much smaller species such as proteins. All these words describe results of the competition between attractive forces, electrostatic interactions, and transport by diffusion.) Thus, one can think that during filtration of a colloidal suspension through a thin film, surface interactions play a significant role on the control of material deposition (fouling).

McDonogh et al. (1989) report important variations in the limiting permeate flux in ultrafiltration of latex particles of different surface charges. It is also well known that pH, which changes protein charges, affects the efficiency of ultrafiltration (Fane et al., 1983) and the extent of fouling (Aimar et al., 1986). Our experiments show that the kinetics of deposition of a colloidal clay on an ultrafiltration membrane depends on the suspension salinity. This article explains such a behavior by a theoretical model and quantifies the contribution of surface interactions on transport phenomena to the membrane.

Theoretical Background

Interactions between colloid surfaces involve essentially three different types of forces [DLVO (Derjaguin, Landau, Verwey, Overbeek) theory]: electrostatic double-layer (EDL) interaction, van der Waals attraction, and Born repulsion. These forces depend on the distance between the surfaces and electrostatic double-layer interactions, and depend on surface charge (or potential) and ionic strength. van der Waals forces predominate at small and large interparticle distances, whereas double-layer repulsion dominates at intermediate distances. In general, the interaction potential profile shows a potential barrier which prevents particles from coagulation. The presence of electrolytes in the suspension reduces this barrier. This leads to defining a critical concentration in electrolytes for coagu-
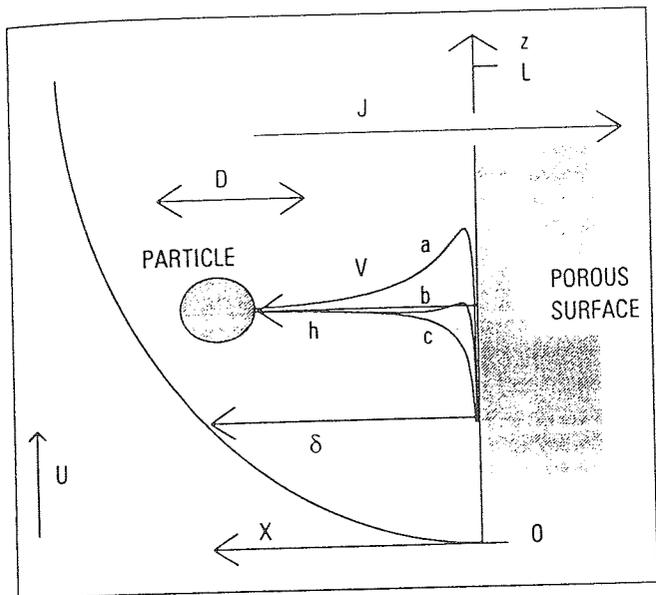
Figure 1. Colloidal particle suspended in a fluid permeating through a porous surface in the presence of a tangential flow.

Factors influencing the transport of the particle are the flux of permeation, J, the diffusion coefficient, D, the interaction energy between the particle and the wall, V, and the tangential flow, U, creating the boundary layer of thickness, δ.

lation representing the transition (curve b in Figure 1) between stability (curve a) and rapid coagulation (curve c). This approach, however, does not take into account transport by diffusion. More rigorous works describing coagulation solve the transport equations with diffusion and interactions induced migration for two spheres. Hence, Verwey and Overbeek (1948) define the rate of coagulation as the rate of diffusion divided by a stability ratio W_c such that:

$$W_c = 2 \cdot a \cdot \int_{2a}^{\infty} e^{\frac{V}{kT}} \frac{dR}{R^2} \qquad (1)$$

where V is the interaction potential energy between two spheres of radius, a, with a distance between their centers, R. W_c is a measure of the effectiveness of a potential barrier in preventing the particle suspension from coagulating or is the reciprocal of a collision efficiency. A value of W_c larger than 10^5 characterizes a stable system (insignificant coagulation) and a stability ratio close to 1 describes a fast coagulation (Smoluchowski, 1917) or an unstable system.

Fouling of a membrane is the result of a combination of solute or particles mass transport to the membrane (deposition) and of solvent transport through the membrane and the deposit layer (filtration). The experimental stationary flux for which there is no solute deposition is the consequence of the first mechanism. The film model describes this stationary state in the case of a membrane totally impermeable for solute by considering a balance across a hydrodynamic diffusion layer between diffusion from the membrane to the solution and convection. This model tends to underestimate the flux obtained experimentally in the case of particles larger than 0.1 μm. This problem, emphasized by Green and Belfort (1980),

is called "colloidal flux anomaly." Several phenomena are invoked to explain this anomaly: shear induced particle diffusion (Zydney and Colton, 1986; Romero and Davis, 1988) or lateral migration (Porter, 1972; Green and Belfort, 1980). These models, essentially based on hydrodynamics, do not predict the changes observed in filtration with the physicochemical properties of suspension (such as pH or ionic strength). On the other hand, particle deposition on collectors, also very dependent on attractive (barrierless deposition) or repulsive surface interactions (barrier controlled deposition) (Adamczyk, 1989) is described by numerous models (Jia and Williams, 1990) accounting for specific surface interactions between the particles to be deposited and the charged solid-liquid interface. In the case where interactions between particles in the bulk can be neglected (This assumption implies that the concentration does not affect physicochemical properties of the suspension. To overcome this assumption, the full Fokker-Planck equation must be used.), the governing equation is the continuity equation (Eulerian approach):

$$\frac{dc}{dt} + \nabla N = Q \qquad (2)$$

where c is the colloid concentration, Q is the bulk reaction term, and N is the mass flux. The steady-state equation, in the absence of bulk reaction is then:

$$\nabla N = 0 \qquad (3)$$

The mass flux can be written as follows as a sum of fluxes due to liquid flow (a), diffusion (b), and interactions induced migration (c):

$$N = u \cdot c - D \cdot \nabla c - \frac{D}{kT} \cdot c \cdot \nabla V \qquad (4)$$
$$\text{(a)} \qquad \text{(b)} \qquad \text{(c)}$$

Here, D is the diffusion coefficient, V is the interaction potential between the particle surface and the collector, k is the Boltzmann constant, T the absolute temperature, and u the hydrodynamic velocity of the fluid. The boundary condition mostly used is the "perfect sink" condition originally applied by Smoluchowski (1917) to describe fast coagulation and later by Verwey et Overbeek (1948) to derive Eq. 1:

$$x = 0 \quad c = 0 \qquad (5)$$

Thus, the basic assumption is that all particles arriving at the collector surface are irreversibly and quickly captured and disappear from the system. Systematic studies of the influence of the shape of interaction profile on particle deposition kinetics have been made by numerical computations of transport equations on rotating disc (Rajagopalan and Kim, 1981) or on a stagnation point flow (Chari and Rajagopalan, 1985).

A lot of models developed considering surface interactions describe deposition of colloids on different types of collectors. To our knowledge, however, this approach has not been applied to the calculation of mass transfer onto a porous surface, such as a membrane in operation.

Model Development

Our model uses the Eulerian approach based on the continuity equation (Eq. 3). The transport equation (Eq. 4) is modified by considering a fluid velocity near the interface due to the sole permeate flux, J (term (a) equal to Jc). The tangential flow is taken into account to calculate the diffusion layer thickness for any point of the membrane surface (Figure 1). If we consider that all the mass transport occurs within the limits of the hydrodynamic layer then:

$$x = \delta \quad c = c_0 \qquad (6)$$

A first boundary condition is given by the perfect sink model (Eq. 5) applied to the moving solid-liquid interface constituted by the cake top surface. Considering a constant diffusion coefficient, this equation system (Eqs. 3, 4, 5 and 6) leads to the following analytical solutions for concentration profile and rate of mass transfer:

$$c = c_0 \cdot e^{-\frac{V}{kT} - \frac{J}{D}(h-\delta)} \frac{\int_0^h e^{+\frac{V}{kT} + \frac{J}{D}x} \cdot dx}{\int_0^\delta e^{+\frac{V}{kT} + \frac{J}{D}x} \cdot dx} \qquad (7)$$

$$N = \frac{D \cdot c_0 \cdot e^{\frac{J\delta}{D}}}{\int_0^\delta e^{+\frac{V}{kT} + \frac{J}{D}x} \cdot dx} \qquad (8)$$

Calculations of c and N by these stiff equations are rather complex. A simplification of Eq. 8 is possible by considering that the surface interaction occurs across a layer (a few nanometers) thinner than the hydrodynamic layer ($1-10\,\mu m$). The mass-transfer Eq. 8 can then be simplified and written in a dimensionless form:

$$Sh = \frac{1}{\frac{V_B}{\delta} e^{-Pe} + \frac{1}{Pe}(1 - e^{-Pe})} \qquad (9)$$

with

$$Sh = \frac{N \cdot \delta}{D \cdot c_0} \qquad (9a)$$

$$Pe = \frac{J \cdot \delta}{D} \qquad (9b)$$

$$V_B = \int_0^\infty (e^{\frac{V}{kT}} - 1) \cdot dx \qquad (9c)$$

The mass transfer, Sh, is expressed as a function of hydrodynamic conditions, Pe and δ, and of physicochemical properties V_B, representing the potential barrier induced by the surface interactions.

Definition of stability for deposition, W_d

A limit to general Eq. 9 is the case of a Pe number close to zero (nonporous surface or negligible applied pressure). The deposition or the adsorption of colloids on such a surface with a tangential flow is then given by:

$$Sh = \frac{1}{1 + \frac{V_B}{\delta}} \qquad (10)$$

Mass transfer is then limited by a combination of a diffusion resistance and of a resistance to transport induced by interactions. In a dimensional form, the potential barrier reduces the flux by an apparent increase in the diffusion layer thickness (This equation is similar with the Ruckenstein and Prieve (1973) analysis of colloid deposition on a plane under parallel flow conditions. Thus, the dimensionless number, V_B/δ, can be linked with a Damköhler number as the ratio of a surface reaction rate defined by these authors on a diffusion rate, $V_B/\delta = 1/Da$):

$$N = \frac{D}{\delta + V_B} \cdot c_0 \qquad (11)$$

The rate of deposition can be written as a mass transfer by diffusion, $D(c_0-0)/\delta$, divided by a ratio, W_d, characterizing the stability of a single particle with respect to the membrane surface swept by a cross flow:

$$W_d = 1 + \frac{V_B}{\delta} \qquad (12)$$

Equation 12 then defines a criterion for the effectiveness of a potential barrier, V_B, and of hydrodynamics, δ, in preventing the suspension from deposition. As for coagulation (Eq. 1), a value of W_d around one (in the absence of interaction: $V_B = 0$) corresponds to deposition only by diffusion, whereas a large ratio (large repulsion interactions: $V_B \gg 0$) represents cases of negligible deposition. The stability decreases for a decreasing cross-flow velocity in the case of repulsive interactions $V_B > 0$ (shear enhanced particle removal) and for increasing velocity in the case of attractive interactions, $V_B < 0$, (shear induced particle deposition). The stability W_d (Eq. 12) can be compared to the stability defined for coagulation, W_c (Eq. 1) which can be expressed, for large potential barriers and using Eq. 9c, as follows:

$$W_c = 1 + \frac{V_B}{2a} \qquad (13)$$

Thus, if one assumes a boundary layer thickness such as $1\,\mu m$, a particle with a diameter of $1\,\mu m$ would have the same value of W_c and W_d. On the other hand, a solute of 10 nm in diameter (such as a protein) in a boundary layer of $1\,\mu m$ has a stability W_d 100 times smaller than its stability with respect to coagulation. Such a solution could then be stable in solution but prone to deposit or adsorb on a surface.
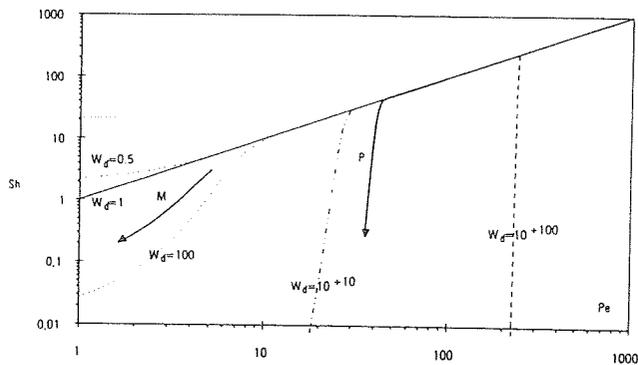
Figure 2. Deposition, *Sh*, vs. convection, *Pe*, for different stability values, W_d.

Bold lines represent fouling paths for a macromolecule (*M*) or a colloidal particle (*P*) (data from Table 1).

Discussion of the Model

The combination of the transfer equation (Eq. 9) and of the relationship defining the stability, W_d, (Eq. 12) leads to:

$$Sh = \frac{1}{(W_d - 1)e^{-Pe} + \frac{1}{Pe}(1 - e^{-Pe})} \tag{14}$$

Equation 14 has been plotted in Figure 2 for different values of the stability, W_d. For low diffusivity and a negligible potential barrier ($V_B = 0$ and $W_d = 1$), all the material brought by convection is deposited on the surface: this is dead-end filtration ($Sh = Pe$). In the case of attractive interactions ($V_B < 0$ and $W_d < 1$), the transfer is larger than the mass brought by convection ($Sh > Pe$). This difference is due to physical adsorption which gains more and more importance as convection becomes smaller (decreasing Pe). During filtration, the attractive interactions case can only be a transient one as the membrane is soon covered by a particle layer. For a repulsive potential barrier ($V_B > 0$ and $W_d > 1$), which is often the case in filtration (interaction between suspended particle and cake of particle), the Sherwood number is smaller than the Pe number: the repulsive interaction creates an additional resistance to mass transfer towards the surface. This resistance decreases when the Pe increases. For large Pe numbers, $Sh = Pe$. The transition zone between Pe for which $Sh < Pe$ and Pe for which $Sh = Pe$ is sharper when the potential barrier increases. For large values of W_d, it exists a critical value of Pe below which

the potential barrier makes the deposition almost impossible ($Sh = 0$) and above which fouling is maximum ($Sh = Pe$). Such a phenomenon is common to all collectors (Chari and Rajagopalan, 1985), as well as to coagulation. In the case of filtration with important repulsive interactions this trend would lead to consider, for given hydrodynamic conditions, a threshold flux below which no fouling would occur.

Implication for membrane fouling

Typical values of Pe and V_B/δ obtained for two very different classes of colloids (a protein, bovine serum albumin (BSA), and a particle of larger size, bentonite) are presented in Table 1. The brownian diffusion for particles is smaller than for small solutes like BSA and thus, for the same permeate flux and hydrodynamic conditions, the Pe number is much larger for the particle than for the protein. The size has an important effect on the surface interaction between particles, the potential barrier for a particle being several orders of magnitude larger than for the protein, for the same surface conditions. The dimensionless numbers Pe and V_B/δ are then helpful in comparing different colloids from a stability and fouling point of view. According to Eq. 9, once these values are known, it is possible in principle to determine the mass transfer, Sh. Sh/Pe is the ratio of mass transfer, N, to convection, Jc. This number can be considered as an index of the "fouling potential": a value of 1 characterizes a fouling situation as observed in dead-end filtration, a ratio of 0 corresponds to negligible fouling and a ratio larger than 1, fouling enhanced by adsorption. Figures 3 and 4 present contours of this "fouling potential" (constant Sh/Pe) in a graph representing the suspension characteristic, W_d, (Eq. 12) vs. the Pe.

In the "particle" case (large Pe and W_d as in Figure 3), the transition between "no fouling" and "dead-end fouling" zones is very sharp and monotonous. An analytical approximation for the boundary of the no-fouling condition was found to be:

$$Pe_{crit} \approx \ln\left(\frac{V_B}{\delta}\right) \tag{15}$$

This equation in good agreement with iso-fouling curves (Figure 3) leads to the determination of a threshold flux below which no fouling occurs. This flux is a function of the properties of the colloid and of the suspension, V_B and D, and of the hydrodynamics, δ. The concept of threshold flux has often been discussed. Cohen and Probstein (1986) have reviewed the major mechanisms describing such a phenomenon: back flux

Table 1. Estimated Dimensionless Numbers in Eq. 9 for Two Very Different Colloids: Clay and Protein

Colloids	*a* (nm)	D^* (m²/s)	δ^{**} (m)	$V_B^\dagger$ (m)	$Pe^\ddagger$	V_B/δ
"Particle" Bentonite	350	6.3×10^{-13}	1×10^{-6}	$1 \times 10^{+10}$	200	$1 \times 10^{+16}$
"Macromolecule" BSA	3.6	6×10^{-11}	4.3×10^{-6}	1×10^{-4}	10	20

*Calculation of diffusion coefficient by Stokes Einstein law, $D = kT/6\pi\mu a$.
**Calculation of diffusion layer thickness by Lévêque equation: $d_h/\delta = 1.62 [Re \cdot Sc (d_h/L)]^{0.33}$ with $Re = 800$, $Sc = \mu/\rho D$ and $\mu/\rho = 1 \times 10^{-6}$ (Pa·s·m³/kg), the hydraulic diameter $d_h = 5 \times 10^{-4}$ m and the membrane length $L = 0.3$ m.
†Calculation of the potential barrier (Eq. 9c) with unretarded van der Waals interaction (Hamaker constant = 1×10^{-20} J): for bentonite, constant charge double layer interaction (Wiese and Healy, 1970) with $I = 0.003$ M and $\zeta = -40$ mV; for BSA, approximation of Stitger and Hill (1959) with $I = 0.003$ M and charge -6.8 in electronic charge as used by Anderson et al. 1978).
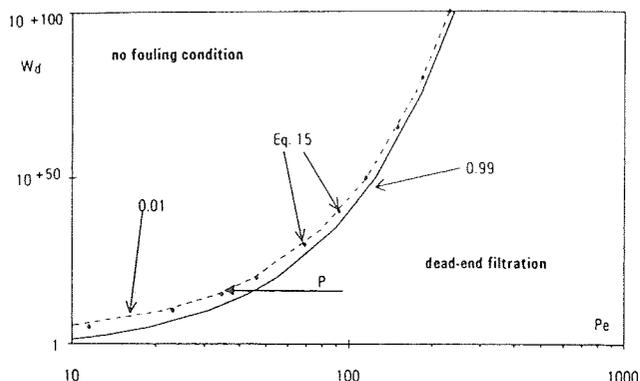‡Calculation of Peclet number with initial permeate flux of 6.3×10^{-5} m/s.

Figure 3. Stability, W_d, vs. convection, Pe, for different fouling potentials, Sh/Pe, (particles case).

Equation 15 (◆) is a good approximation for the limit of the no fouling condition. Bold line represents the simulated fouling path during particle filtration.

by diffusion, lateral migration, and shear induced diffusion. These existent theories are compared to interaction enhanced migration (present model) in Table 2 and in Figure 5 as a function of solute size. Interaction enhanced migration (Eq. 15) gives larger threshold fluxes for colloids with size between 0.1 and 10 μm than classical models and then can provide an explanation for the "colloidal flux anomaly." This mechanism can explain the experimental observation by Cohen and Probstein (1986) of an essentially constant threshold flux for reverse osmosis of colloidal suspension (ferric hydroxide RO with size between 0.1 and 0.5 μm represented by black squares in Figure 5). For particles larger than 10 μm, hydrodynamic mechanisms seem the most important and for colloids smaller than 0.1 μm, Brownian diffusion induces a back flux larger than interaction enhanced migration but can also lead to adsorption.

In the case of macromolecules, the isofouling graph (Figure 4) is more complex than before. High diffusivity and small potential barrier make the adsorption mechanism possible. Thus, there are now three different zones (adsorption, dead-end filtration and no-fouling conditions) and a large transition area between these zones. An important point is that for low
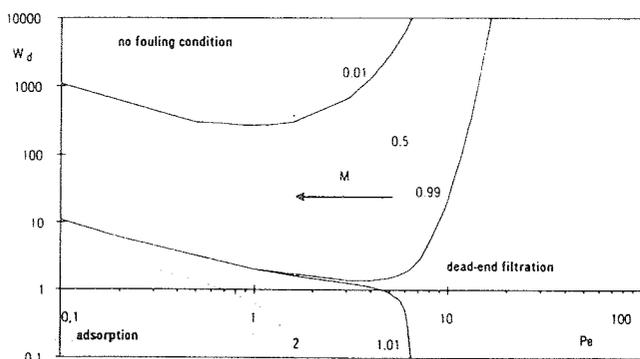

Figure 4. Stability, W_d, vs. convection, Pe, for different fouling potentials, Sh/Pe (macromolecules case).

Bold line represents the simulated fouling path for simulation during macromolecule solution filtration.

Table 2. Mechanisms Explaining a Critical Flux in UF, MF or RO of Large Colloids

Mechanism	Expression
Brownian Diffusion	$j_d = D/\delta = (1/\delta)(kT/6\pi\mu a)$
Shear Enhanced Diffusion	$j_s = D_s/\delta = (1/\delta)\,(0.2Ua^2/d_h)$
Lateral Migration	$j_l = 4U^2a^3/\nu d_h^2$
Interaction Induced Migration	$j_v = (D/\delta)\cdot\ln(V_B/\delta)$ (This Work)

values of W_d (<100), there is no stationary flux predicted here. A fraction of the mass transport (adsorption, Eq. 10) is independent of Pe, and then gains more and more importance in Sh/Pe as Pe decreases. For W_d large enough, Figure 4 shows a no fouling zone. This model accounts for the variations in permeation flux for protein ultrafiltration observed by Fane et al. (1983) at different pH and ionic strengths as V_B depends on the surface charge and ionic strength. For example, a minimum of threshold permeate flux, and a maximum fouling, observed at the isoelectric point cannot be predicted by the variations in osmotic pressure with pH. It can be explained by weaker interaction induced migration (present model) when the molecule net charge is near zero, as well as by a lower solubility at IEP (gel model).

Some properties of proteins, however, are not yet accounted for by the present model (osmotic pressure, solubility, hydrophobic interaction, or denaturation). Furthermore, if concentration plays a role on the rate of membrane fouling in Eq. 16, it has no direct effect on the steady state, as shown by Eq. 15. This comes from the fact that interactions between particles in suspension have been neglected. Then, an improvement to the model, which is for the moment more appropriate for the description of dilute suspensions of large colloids, can be the study of the influence of colloid concentration on physico-chemical properties (stability and diffusion) of the suspension and then on fouling.
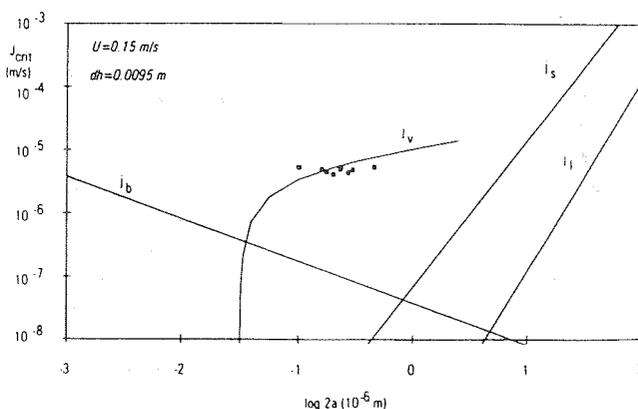

Figure 5. Critical fluxes predicted by different mechanisms vs. particle-size: Brownian diffusion, j_b, lateral migration, j_l, shear induced diffusion, j_s, and interaction induced migration, j_v (Table 2).

Symbols represent threshold fluxes observed during ferric hydroxide RO by Cohen and Probstein (1986). Interaction induced migration, j_v (Eq. 15) calculated with constant potential double layer interaction (Wiese and Healy, 1970) and unretarded van der Waals attraction: ionic strength 0.001 M, Hamaker constant $I \times 10^{-20}$ J and zeta potential 50 mV.

Simulations of membrane fouling

Colloidal fouling of MF, UF and RO membranes is a combination of a transfer mechanism to the surface and of a filtration mechanism through the deposited material and through the membrane. To describe permeate flux in such processes, the transfer equation (such as Eq. 9) is coupled with a cake filtration law presented here in a dimensionless form:

$$Pe = \frac{Pe_0}{1 + \frac{1}{2 \cdot t_{\frac{\sqrt{2}}{2}}} \cdot \frac{\int_0^t Sh \cdot dt}{Pe_0}} \qquad t_{\frac{\sqrt{2}}{2}} = \frac{\Delta P}{2 \cdot \alpha \cdot c_0 \cdot J_0^2} \qquad (16)$$

Here, $t_{\sqrt{2}/2}$ is the characteristic time of dead-end filtration for which the initial permeate flux has been divided by $\sqrt{2}$. Equation 9 allows to calculate the mass transport for a permeate flux at a given time and for a boundary layer thickness, which depends on the location on the membrane surface. Simulation of membrane fouling needs iterative calculations of Eqs. 9 and 16 over the membrane surface and over the process duration. The major assumptions made to derive this model are:

- Cake filtration (no pore blocking) with homogeneous cake properties (no compressibility across the cake thickness) and without osmotic pressure.
- No difference made between the deposition of the first layer (membrane/particle interaction) and further layers (particle/particle layer interaction).
- No effect of concentration on interactions and on diffusion.

It is clear that these assumptions are of importance for the simulation of ultrafiltration of protein solutions and have to be overcome to obtain reliable predictions. These simulations, however, allow the effect of the suspension properties on the kinetics of deposition during membrane fouling to be studied. Different simulations of filtration are discussed below for two different colloids.

In the case of particles (data from Table 1), the simulation shows a stationary flux rapidly obtained after a period of dead-end filtration (Figure 6). This is easily explained by the fouling path, P, resulting of this simulation in Figure 3. In this figure, the beginning of a membrane operation is characterized by a point (stability and Pe number). As the run proceeds, the point shifts horizontally (constant W_d) from right to left (Pe decreasing with membrane fouling). For the particle filtration, the run starts in the zone where the fouling potential, Sh/Pe, is equal to 1 (dead-end filtration) and then rapidly reaches the "no fouling" zone (stationary flux). This trend is also illustrated in Figure 2 where the fouling path, P, begins on the line, $Sh = Pe$, and soon after becomes vertical (almost constant Pe: stationary flux). Furthermore, this threshold flux due to a migration induced by interaction, independent of the applied pressure, explains the trend observed when increasing the pressure in UF or MF (Gourgues et al., 1992). Once a stationary flux has been reached, a stepwise increase in pressure increases the permeate flux: the operating point in Figure 3 gets temporarily away from the stationary flux curve and falls into the dead-end filtration zone; soon the flux diminishes again until the same stationary flux has been reached. The "no deposi-
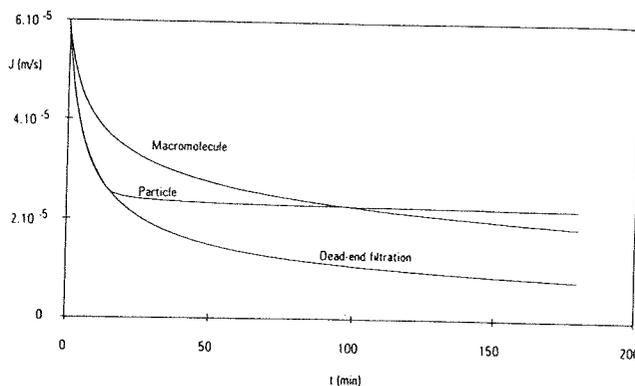

Figure 6. Variation in permeate flux vs. time for typical particles suspensions and proteins solutions (from Table 1).

tion" conditions observed by Gourgues et al. (1992) are also predicted by the present model as mentioned before.

In the case of macromolecules, simulation of solution filtration (Table 1) shows no steady-state, but a slowly declining, flux (Figure 6). This is due to the fact that the fouling path (M in Figure 4) approaches an adsorption zone, which induces a continuous cake growth. This can also be seen in Figure 2 where the fouling path for this simulation (M) stays near the line $Sh = Pe$ (deposition always important as compared to Pe). This simulation is in good agreement with observations made during UF or MF of protein solutions, which are generally characterized by a continuous flux decline.

Application of the Model

Ultrafiltration of latex with different surface charge

McDonogh et al. (1989) performed experiments with latex particles ($a = 12$, 1 nm) of different zeta potentials and under various hydrodynamic conditions. They show that the limiting
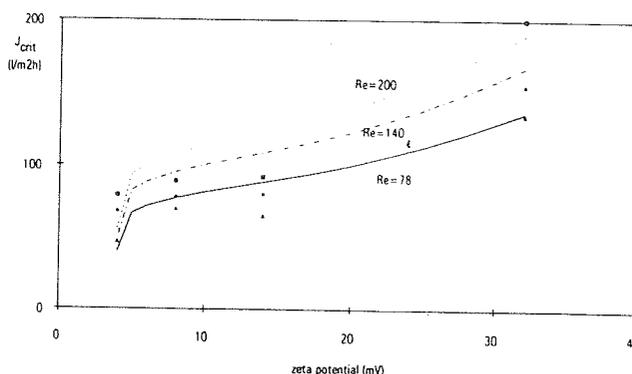

Figure 7. Critical flux, J_{crit}, vs. zeta potential for various Reynolds numbers.

Symbols represent experimental data with latex (McDonogh et al., 1989) and lines calculations with Eq. 15. Calculations with constant potential double layer interaction (Wiese and Healy, 1970) and the unretarded van der Waals attraction and with data: $a = 12.1$ nm, ionic strength 0.001 M, Hamaker constant $I \times 10^{-20}$ J and hydraulic diameter $d_h = 3.22 \times 10^{-4}$ m.
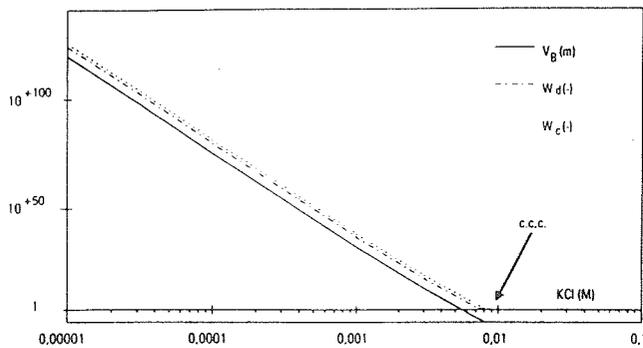
Figure 8. Potential barrier, V_B, vs. ionic strength for a sphere plane configuration.

Calculation with constant charge double layer interaction (Wiese and Healy, 1970) and the unretarded van der Waals attraction, as detailed in Table 1. Value of stabilities, W_d (Eq. 12) and W_c (Eq. 13) with $\delta = 1.5 \times 10^{-5}$ m and $a = 350$ nm.

Figure 9. Adhesion constant K (Eq. 17) vs. KCl concentration.

(— · —) experimental data; (———) calculation (Eq. 18).

UF flux increases when the particles charge increases (Figure 7). Equation 25 and calculations of interactions (data in legend of Figure 7) allow the observations of these authors to be calculated. Variations in limiting flux with surface charge, as well as with hydrodynamic conditions, are in good agreement with experimental data as shown in Figure 7.

Ultrafiltration of bentonite with different salt concentrations

The model was also applied to experiments performed in cross-flow UF of clay (bentonite) with various concentrations of electrolytes. The particles have a mean diameter of 0.7-μm and a -40-mV zeta potential, constant with pH and ionic strength. At low ionic strength, bentonite is stable in suspension but a concentration of 10^{-2} M in KCl leads to a fast coagulation. This critical coagulation concentration c.c.c. is comparable to the one obtained by calculation of stability W_c (Eq. 1) in Figure 8.

Suspensions are made with 0.3 g/L of bentonite in a saline KCl solution (same procedure as Gourgues et al., 1992). The parameter is the concentration of KCl in the suspension, the other operating conditions being constant (applied pressure 100 kPa and average tangential velocity 0.088 m/s). The membranes are outer skinned hollow fibers with a cutoff of 300 kDa (impermeable to this colloid) and have a water permeability of 5×10^{-10} m/(s·Pa). The shell is 17.8 mm in hydraulic diameter and contains 24 hollow fibers spaced enough for hydrodynamic interactions between two fibers to be neglected. Experiments have been performed in a unit allowing continuous measurement of the permeate flux and of the bulk concentration in retentate. Simple mass balance then allows the amount of particles deposited on the membrane to be worked out (Gourgues et al., 1992). These measurements allow the calculations of the specific resistance of the cake, α, and of the kinetic deposition parameter, J_{crit}, to be performed.

Circulating the suspension in the UF loop without permeation reveals a bulk concentration reduction, explained by an adhesion mechanism. Such experiments have been performed at various ionic strengths to determine a kinetics constant, K,
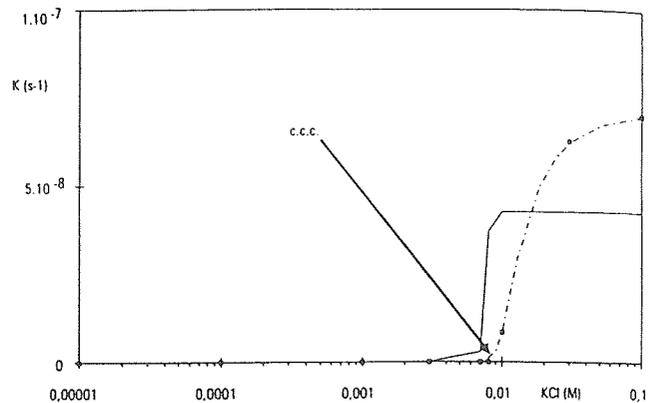
as adhesion is generally described by a first-order reaction (Tamaï et al., 1982):

$$\frac{dc}{dt} = K \cdot c \tag{17}$$

This mechanism, once quantified, has been accounted for in calculating the critical flux.

Adhesion appears for a salt concentration around c.c.c. (Figure 9). This rapid mechanism is often observed and allows a critical deposition salt concentration to be determined (van de Ven, 1989). These variations are modeled by Eq. 11 derived for deposition on a nonporous surface. By combining a theoretical equation (Eq. 11) and an experimental kinetics (Eq. 17), one can derive the following expression:

$$K = \frac{S}{Vo} \cdot \frac{D}{\delta \cdot W_d} \tag{18}$$

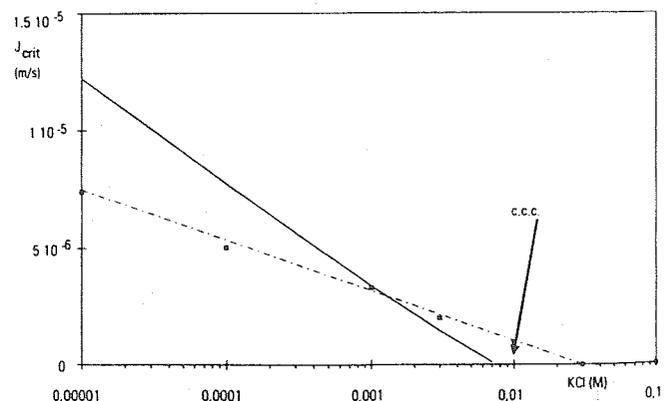Assuming the ultrafiltration apparatus is a collector with the

Figure 10. Critical flux, J_{crit} as a function of KCl concentration.

(— · —) experimental data; (———) calculated data (Eq. 15).

same properties as those of a bentonite surface give data which are in good agreement with experimental results (Figure 9).

As can be seen from Figure 10, the other parameter of deposition kinetics, J_{crit}, is greatly influenced by KCl concentration. At low ionic strength, a large critical flux is observed. Addition of salt results in a lower limiting flux and a larger deposition on the membrane. For ionic strength close to c.c.c., this limiting flux is almost zero: the amount of material deposited on the surface is equal to the amount brought by convection (dead-end filtration). This parameter, J_{crit}, can be compared with the value predicted by relation 15. Calculated values (data from Table 1) show the same type of variation as experimental data in Figure 10. The model explains reductions in critical flux when the salt concentration is increased by shielding the electrostatic repulsion between the cake surface and the approaching charged particles. A quantitative agreement is not achieved, but the theoretical model of a bentonite particle as a hard sphere is certainly too far from reality to provide exact predictions. Another model based on a platelet geometry was tried, however this was not successful either.

Conclusions

A theoretical equation has been derived to describe the rate of a colloid deposition to a porous surface in cross-flow conditions, as a function of hydrodynamic conditions and suspension properties such as diffusivity and stability. The transfer equation shows how the concept of stability ratio of a suspension is an important characteristic for membrane fouling as well as for particle aggregation.

For filtration of large charged particles, this equation explains the existence of a threshold flux, J_{crit}, due to interaction induced migration:

$$J_{crit} = \frac{D}{\delta} \cdot \ln\left(\frac{V_B}{\delta}\right)$$

where the boundary layer thickness, δ, characterizes hydrodynamics conditions and the particle diffusivity, D, and the potential barrier between particles induced by surface interactions V_B (linked to suspension stability and to tangential flow by Eqs. 12 and 13) account for the physicochemical properties of the suspension. This threshold flux is the edge between pure dead-end filtration (where convection overcomes surface repulsion) and nonfouling (where surface repulsion dominates). The present model predicts a higher flux than other models in the range of colloid size 0.1 to 10 μm and might then contribute to solve the "colloidal flux anomaly." It gives results in good agreement with measurements on latex ultrafiltration (McDonogh et al., 1989), ferric hydroxide reverse osmosis (Cohen and Probstein 1986), or clay ultrafiltration (this work).

For smaller solutes, that is, macromolecules, the model predicts a more complex situation with physical adsorption occurring at low stability and low Pe number. The model predicts the continuous flux decline observed for UF or MF of proteins, and the variations in membrane fouling with ionic strength and pH, although it does not yet include several important physicochemical properties of protein solutions.

Notation

a = particle radius, L
c = colloid concentration, $M \cdot L^{-3}$
c_0 = bulk concentration, $M \cdot L^{-3}$
d_h = hydraulic diameter, L
D = diffusion coefficient, $L^2 \cdot T^{-1}$
h = separation distance between particle and surface, L
J = permeate flux, $L \cdot T^{-1}$
J_0 = initial permeate flux, $L \cdot T^{-1}$
J_{crit} = critical or threshold flux defined in Eq. 15, $L \cdot T^{-1}$
N = mass flux, $M \cdot L^{-2} \cdot T^{-1}$
P = pressure, $M \cdot L^{-1} \cdot T^{-2}$
Pe = Peclet number: ratio convection/diffusion
Pe_0 = Peclet number at the beginning of filtration
Pe_{crit} = threshold Peclet number defined in Eq. 15
Sc = Schmidt number, ν/D
Sh = Sherwood number: ratio mass transfer/diffusion
t = time, T
T = temperature, K
U = velocity of fluid tangential to the membrane, $L \cdot T^{-1}$
V = total potential energy of interaction, $M \cdot L^2 \cdot T^{-2}$
V_B = value of potential barrier defined in Eq. 9c, L
V_0 = volume of solution in UF unit, L^3
W_d = stability ratio of suspension with respect to deposition on a surface in cross-flow conditions

Greek letters

α = specific resistance of the cake deposited on the membrane (Eq. 16), T^{-1}
δ = boundary layer thickness, L
μ = solvent viscosity, $M \cdot L^{-1} \cdot T^{-1}$
ρ = solution density $M \cdot L^{-3}$

Literature Cited

Adamczyk, Z., "Particle Deposition from Flowing Suspensions," *Colloids and Surf.*, 39, 1 (1989).

Aimar, P., S. Baklouti, and V. Sanchez, "Membrane-Solute Interactions: Influence on Pure Solvent Transfer During Ultrafiltration," *J. Memb. Sci.*, 29, 207 (1986).

Anderson, J. L., F. Rauh, and A. Morales, "Particle Diffusion as a Function of Concentration and Ionic Strength," *J. Phys. Chem.*, 82(5), 608 (1978).

Chari, K., and R. Rajagopalan, "Deposition of Colloidal Particles in Stagnation Point Flow," *J. Chem. Soc. Farad. Trans.*, 2(81), :345 (1985).

Cohen, R. D., and R. F. Probstein, "Colloidal Fouling of Reverse Osmosis Membranes," *J. Colloid Interf. Sci.*, 114(1), 194 (1986).

Fane, A. G., C. D. J. Fell, and A. G. Waters, "The Effects of pH and Ionic Environment on the Ultrafiltration of Protein Solutions with Retentive Membranes," *J. Memb. Sci.*, 16, 195 (1983).

Gourgues, C., P. Aimar, and V. Sanchez, "Ultrafiltration of Bentonite Suspensions with Hollow Fiber Membranes," *J. Memb. Sci.*, 74, 51 (1992).

Green, G., and G. Belfort, "Fouling of Ultrafiltration Membranes: Lateral Migration and Particles Trajectory Model," *Desalin*, 35, 129 (1980).

Jia, X., and R. A. Williams, "Particle Deposition at a Charged Solid-Liquid Interface," *Chem. Eng. Comm.*, 91, 127 (1990).

McDonogh, R. M., A. G. Fane, and C. J. D. Fell, "Charge Effects in the Cross-Flow Filtration of Colloids and Particulates," *J. Memb. Sci.*, 43, 69 (1989).

Porter, M. C., "Concentration Polarization with Membrane Ultrafiltration," *Ind. Eng. Chem. Prod. Res. Dev.*, 11, 234 (1972).

Rajagopalan, R., and J. S. Kim, "Adsorption of Brownian Particles in the Presence of Potential Barriers: Effect of Different Modes of Double Layer Interaction," *J. Colloid Interf. Sci.*, **83**, 2 (1981).

Romero, C. A., and R. H. Davis, "Global Model of Cross Flow Microfiltration Based on Hydrodynamic Particle Diffusion," *J. Memb. Sci.*, **39**, 157 (1988).

Ruckenstein, E., and D. C. Prieve, "Rate of Deposition of Brownian Particles Under the Action of London and Double Layer Forces," *J. Chem. Soc. Farad. Trans.*, 2(69), 1522 (1973).

Smoluchowski, M. von, "Mathematical Theory of the Kinetics of the Coagulation of Colloidal Solutions," *Z. Phys. Chem.*, **92**, 129 (1917).

Stigter, D., and T. L. Hill, "Theory of the Donnan Membrane Equilibrium II. Calculation of the Osmotic Pressure and of the Salt Distribution in a Donnan System with Highly Charged Colloid Particles," *J. Phys. Chem.*, **63**, 551 (1959).

Tamai, H., and T. Suzawa, "Latex Deposition on Fibers: Effect of Electrolytes on Rate and Interaction Energy," *J. Colloid Interf. Sci.*, **88**, 2 (1982).

Van de Ven, T. G. M., "Effects of Electrolytes, Polymers and Polyelectrolytes on Particle Deposition and Detachment," *Colloids and Surf.*, **39**, 107 (1989).

Verwey, E. J. W., and J. Th. G. Overbeek, *Theory of the Stability of Lyophobic Colloids: The Interaction of Sol Particles Having an Electric Double Layer*, Elsevier, New York (1948).

Wiese, G. R., and T. W. Healy, "Effect of Particle Size on Colloid Stability," *Trans. Farad. Soc*, **66**, 490 (1970).

Zydney, A. L., and C. K. Colton, "A Concentration Polarization Model for the Filtrate Flux in Cross Flow Microfiltration of Particulate Suspension," *Chem. Eng. Comm.*, **47**, 1 (1986).